Bioorganic & Medicinal Chemistry Letters 29 (2019) 1246–1255

Contents lists available at ScienceDirect

Bioorganic & Medicinal Chemistry Letters

journal homepage: www.elsevier.com/locate/bmcl

Synthesis and biological evaluation of Doxorubicin-containing conjugate targeting PSMA

Yan A. Ivanenkov[a,b,c,d,e,*], Alexey E. Machulkin[b], Anastasia S. Garanina[b,c], Dmitry A. Skvortsov[b], Anastasia A. Uspenskaya[b], Ekaterina V. Deyneka[a], Alexander V. Trofimenko[a], Elena K. Beloglazkina[b], Nikolay V. Zyk[b], Victor E Koteliansky[b], Dmitry S. Bezrukov[b,f], Anastasia V. Aladinskaya[a], Nataliya S. Vorobyeva[h], Maria M. Puchinina[a], Grigory K. Riabykh[b], Alina A. Sofronova[i], Alexander S. Malyshev[k], Alexander G. Majouga[b,c,g]

[a] Moscow Institute of Physics and Technology (State University), 9 Institutskiy lane, Dolgoprudny City, Moscow Region 141700, Russian Federation
[b] Lomonosov Moscow State University, Chemistry Dept., Leninskie gory, Building 1/3, GSP-1, Moscow 119991, Russian Federation
[c] National University of Science and Technology MISiS, 9 Leninskiy pr, Moscow 119049, Russian Federation
[d] ChemDiv, San Diego, California, USA
[e] Institute of Biochemistry and Genetics Ufa Science Centre Russian Academy of Sciences (IBG RAS), Oktyabrya Prospekt 71, 450054 Ufa, Russian Federation
[f] Skolkovo Institute of Science and Technology, Skolkovo Innovation Center, Building 3, Moscow 143026, Russian Federation
[g] Dmitry Mendeleev University of Chemical Technology of Russia, Miusskaya sq. 9, Moscow 125047, Russian Federation
[h] Centaura LLC, Moscow, Russia
[i] Lomonosov Moscow State University, Faculty of Bioengineering and Bioinformatics, Moscow, Russian Federation
[k] Lomonosov Moscow State University, Faculty of Medicine, Moscow, Russian Federation

ARTICLE INFO

Keywords:
PSMA
Doxorubicin
Targeted drug delivery
Prostate cancer

ABSTRACT

Prostate-specific membrane antigen (PSMA), also known as glutamate carboxypeptidase II (GCPII), has recently emerged as a prominent biomarker of prostate cancer (PC) and as an attractive protein trap for drug targeting. At the present time, several drugs and molecular diagnostic tools conjugated with selective PSMA ligands are actively evaluated in different preclinical and clinical trials. In the current work, we discuss design, synthesis and a preliminary biological evaluation of PSMA-specific small-molecule carrier equipped by Doxorubicin (Dox). We have introduced an unstable azo-linker between Dox and the carrier hence the designed compound does release the active substance inside cancer cells thereby providing a relatively high Dox concentration in nuclei and a relevant cytotoxic effect. In contrast, we have also synthesized a similar conjugate with a stable amide linker and it did not release the drug at all. This compound was predominantly accumulated in cytoplasm and did not cause cell death. Preliminary *in vivo* evaluation has showed good efficiency for the degradable conjugate against PC3-PIP(PSMA$^+$)-containing xenograft mine. Thus, we have demonstrated that the conjugate can be used as a template to design novel analogues with improved targeting, anticancer activity and lower rate of potential side effects. 3D molecular docking study has also been performed to elucidate the underlying mechanism of binding and to further optimization of the linker area for improving the target affinity.

Introduction

PC is one the most leading malignancy among men resulting in a relatively high mortality rate. Its incidence varies significantly depending on geographic area due to the coverage of PSA screening,[1] but anyhow, approx. 2% of PC patients die. For instance, in 2012, 1.1 million men were diagnosed with PC worldwide (about 15% of all cancer diagnoses), while in Europe this rate was over 400,000.[2] Currently, the American Cancer Society's (ACS)[3] estimates ~164,690 new cases of PC and 29,430 deaths from this disease in the United States for 2018.

Thus, it is the third leading cause of cancer death in American men, behind lung cancer and colorectal cancer. > 12 times higher mortality rate is estimated around the world, where PC represents 7% of total

* Corresponding author at: Moscow Institute of Physics and Technology (State University), 9 Institutskiy lane, Dolgoprudny City, Moscow Region 141700, Russian Federation.
E-mail address: yai@chemdiv.com (Y.A. Ivanenkov).

https://doi.org/10.1016/j.bmcl.2019.01.040
Received 2 October 2018; Received in revised form 15 January 2019; Accepted 30 January 2019
Available online 01 February 2019
0960-894X/ © 2019 Published by Elsevier Ltd.

male cancer mortality.

PSMA is the most attractive biomarker for molecular probe targeting against PC. Thus, PSMA is used as a part of positron emission tomography/computed tomography (PET/CT) where it demonstrates better efficiency for the detection of PC sites than choline PET/CT, especially for patients with low PSA.[4,5] It should be noted, that an elevated level of PSMA expression was observed in other solid tumors thereby promoting their neovasculature and angiogenesis.[6,7]

There are some first-line drug therapy options, e.g.: enzalutamide; degarelix; abiraterone; cabazitaxel[8] which showed significant activity within a life-prolonging chemotherapy for PC; and docetaxel, for patients with PC, including metastatic or/and castration-resistant cases.

It is not surprising that this treatment is often associated with a wide range of side effects, including muscular atrophy, pain, weight changes, and leads to a substantial limitation in health-related quality of life.[9,10] Considering this, alternative therapeutic approaches are currently under active development within this area, for instance, targeted drug delivery with selective PSMA ligands.[11–13] Thus, PSMA-based radioligand therapy (RLT)[4,14] is mainly used as a compassionate treatment after failure of the life-prolonging drugs cited above. For example, lutetium radiolabeled humanized monoclonal antibody (J591) targeting PSMA (^{177}Lu-J591) is being evaluated in Phase II clinical studies in patients with metastatic androgen-independent PC.[15,16] Lutetium-based radionuclide equipped by urea-containing PSMA-targeted core-head ([^{177}Lu]PSMA-617) is in Phase II clinical development for the treatment of patients with metastatic castration-resistant prostate cancer (mCRPC)[17–20] and in Phase II/III against lymph node metastatic PC.[21]

Recently, indotecan-like topoisomerase I inhibitor has been conjugated to the selective PSMA ligand (DUPA) via a peptide linker and a drug-release disulfide trigger that facilitates intracellular cleavage of the delivery system to release the drug molecule within the desired site.[22] This conjugate demonstrated more favorable results *in vivo* than unmodified drug.

The successful story and structural composition of PSMA were described in detail in a range of previous reports,[23,24] so it remains beyond the scope of this paper. Although a considerable progress has been achieved through the past decade within the title field an intrinsic role of PSMA in tumor angiogenesis and carcinogenesis remains mostly uncovered. Anyhow, PSMA has been recognized as one of the most paramount drug targets within the top of modern medicinal chemistry and diagnostics. Therefore, endogenous-like small-molecule ligands specifically targeting PSMA are firmly regarded as a revolutionary and robust tool for the aforementioned therapeutic indications.[25–27]

From the structural point of view, all the ligands and inhibitors of PSMA activity can be roughly divided in three distinct categories: a) antibodies, b) small-molecule compounds, and c) their conjugates. As briefly mentioned above, antibody drug conjugates (ADCs) specifically targeted against PSMA are being under active development in advanced clinical trials.[20,28–31] With respect to anti-androgen therapy, PSMA ADCs have also been evaluated following a concomitant treatment schedule with enzalutamide and abiraterone in LNCaP and C4-2 cells using the Bliss independence method.[32] The theranostic applications of small-molecule high affinity PSMA ligands have been properly regarded as holding great promise for the targeted PC drug therapy and diagnostics.[33–48]

Most of the currently evaluated PSMA-targeted conjugates contain urea-based core-head equipped by a linker of different type and properties as well as by terminal imaging dye to achieve good binding, selectivity and imaging. Several QSAR studies have also been carried out and clearly highlighted the crucial role of Glu-Urea (GU) warhead for a pronounced binding.[49,50] Even though, there is still no such hybrid drug candidate in clinics designed specifically for the targeted PC chemotherapy except EC-1169 (*vide infra*). Several recent conjugates hold great promise as they have successfully passed initial preclinical evaluation. However, the diversity in structure of available PSMA ligands of synthetic origin is a relatively poor and not beyond the scope of three main scaffolds. To the best of our knowledge, GU "anchor" and its isosteric analogues seem broadly sufficient to design novel effective conjugates for drug targeting and PC diagnostics. Here we describe a convenient and versatile synthetic route to novel PSMA ligand equipped by Dox. The activity of the compound was assessed *in vitro* (LNCaP and PC-3 cell lines) using fluorescent microscopy and MTS assay as well as *in vivo* using PIP(PSMA$^+$)-containing xenograft mine. The strategic focus was placed on the spacer length and its nature to achieve an appropriate selectivity and potency.

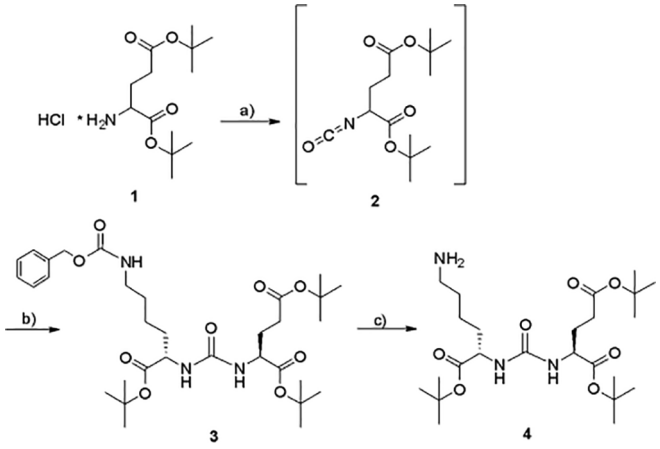

Scheme 1. Synthesis of the starting building **4**: *a)* triphosgene, DIPEA, CH_2Cl_2, − 78 °C; *b)* Cbz-Lys-O(*t*-Bu), DIPEA, CH_2Cl_2, rt, yield 80%; *c)* H_2, 10% Pd/C, CH_2Cl_2, yield 80%

Results

Synthesis

Among a variety of PSMA ligands available to date we selected the urea-based core-head armed by Glu and Lys (GUL) with an IC_{50} value of 498 nM.[51] The decision was made to get the starting materials with a flexible and versatile diversity point that would be easy to modify. The desired conjugates were obtained following the general synthetic approach depicted in Schemes 1–5 below. Initially, compound **4** was readily synthesized from a commercially available *di-tert*-butyl glutamic acid ester **1** in two steps (Scheme 1) via the formation of intermediate isocyanate **2** *in situ* in the presence of triphosgene and DIPEA followed by the reaction with benzyl carbamate protected *tert*-butyl substituted lysine. Subsequent mild hydrogenolysis of **3** with 10% Pd/C furnished the desired product **4** in good yield. Reagents and conditions are listed in the legend.

With respect to the spacer length (*see the Discussion section*), 6-aminohexanoic acid (**5**) and 11-aminoundecanoic acid (**6**) were used as spacer precursors (Scheme 2). Thus, they were initially converted into the Bn-protected derivatives **7** and **8**. The reaction was carried out in toluene with an excess of benzyl alcohol and p-toluenesulfonic acid. The obtained compounds were then immediately reacted with adipic acid monomethyl ester (**9**) resulted in amides **10** and **11**, respectively. Subsequent hydrogenolysis provided two 'mature' linkers **12** and **13** of different length and flexibility. The core-head **4** obtained previously was then readily coupled with these linkers to afford compounds **14** and **15** in good yields. To introduce an appropriate bond labile for endogenously-driven hydrolysis to release a drug specifically within the target tissue, the terminal ester functionality of **14** and **15** was quantitatively converted into the corresponding hydrazides **16** and **17**. The resulting compounds **18** and **19**, bearing convenient link points, were obtained by treating *tert*-Bu esters with 90% TFA in MeOH.

Keeping in mind that aromatic or/and heteroaromatic moieties incorporated into the linker at the most reliable positions (see the

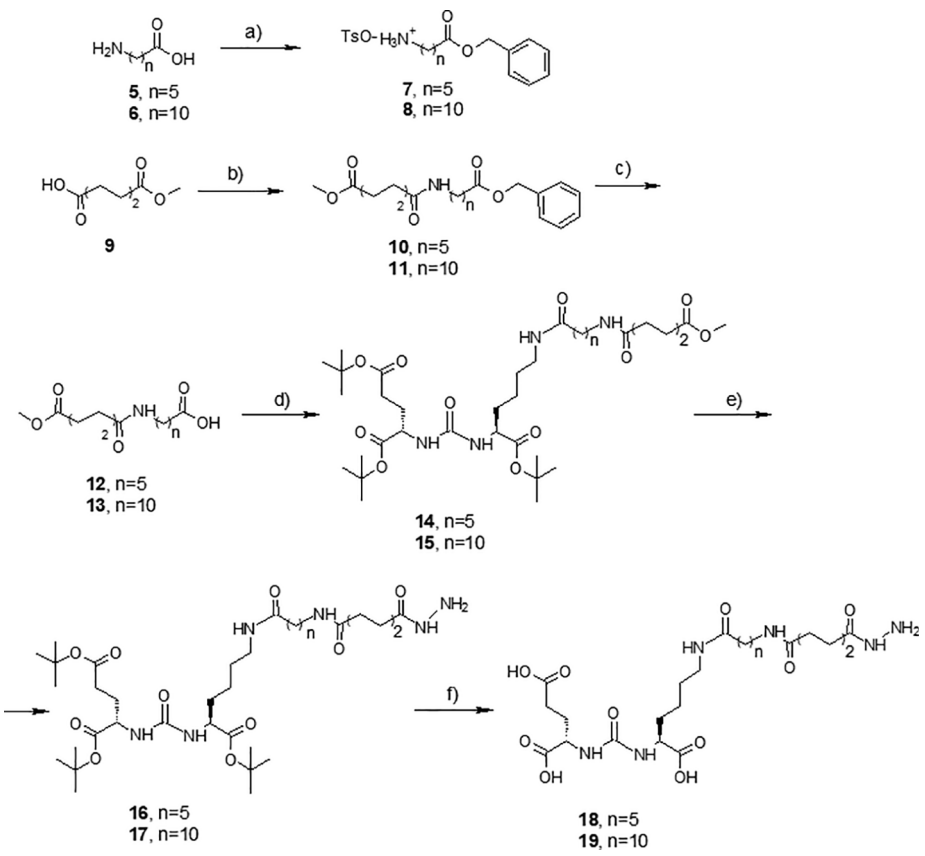

Scheme 2. Synthesis of the carriers **18** and **19**: *a*) $C_6H_5CH_3$, $C_6H_5CH_2OH$, pTsOH, yield **7**–99% **8**–100%; *b*) HBTU, HOBt and DIPEA, yield **10**–64%, **11**–61%; *c*) H_2, 10% Pd/C, MeOH, yield **12**–87%, **13**–100%; *d*) HBTU, HOBt and DIPEA, yield **14**–58%,**15**–63%; *e*) MeOH, Δ, an excess of N_2H_4 H_2O, yield **16**–98%, **17**–96%; *f*) TFA (90%)/MeOH, yield **18**–95%, **19**- quantitative.

discussion below) can significantly improve binding affinity and selectivity, we synthesized the carriers **33** and **34** equipped by two phenylalanine anchors to catch additional supramolecular interactions along the tunnel. Thus, *N*-protected compounds **20** and **21** were treated with the starting material **4** resulted in desired amides **22** and **23** (Scheme 3a). Further hydrolysis furnished corresponding amines **24** and **25** in high yields. The second building block **28** with two phenylalanine fragments was constructed in parallel by the reaction of dipeptide **26** with methanol followed by treating ester **27** with succinic anhydride in DCM at ambient conditions without presence of any base (Scheme 3b). As a result, acid **28** was obtained in good yield and further coupled with amine **24** thereby providing hybrid molecule **29**. Finally, the ester were readily converted into the corresponding hydrazide **30** by analogy to the procedure described above for compounds **16** and **17** (see Scheme 2) and then into the final salt **31**.

In contrast to the approach described by Jayaprakash and coworkers[52] the synthesized hydrazides **18**, **19** and **31** were then conjugated with doxorubicin hydrochloride (Dox) via hydrazone joint that was more susceptible to hydrolysis under the natural environment than pyranose amide bond. The reaction proceeded smoothly in the presence of catalytic amount of trifluoroacetic acid yielding the final products 32–34 (Scheme 4).

To quantitatively estimate the binding potency of the designed carriers towards the title protein we modified compound **25** by fluorescent dye sulfo-Cy5 following the synthetic route depicted in Scheme 5. Thus, the *tert*-Bu ester was readily deprotected in accordance with the method described above for compound **31** (see Scheme 3). The resulting acid **35** was then conjugated with the dye via amide bond and the final product **36** was subsequently purified by HPLC. All the structures of the final products as well as key intermediates were entirely consistent with the ^{1}H NMR and LC-MS spectra (see Supporting Information).

Finally, we synthesized the conjugate **37** following the procedure depicted in Scheme 6. At the first step, Dox was treated with succinic anhydride in the presence of DIPEA in DMF. The reaction mixture was vigorously stirred for 30 min at room temperature then NHS, HBTU and DIPEA were added. The resulting mixture was continuously stirred for several minutes then DIPEA and compound **35** dissolved in DMF were added to the solution and the reaction mixture was further stirred for 30 min. When the reaction was completed (TLC control), the desired compound was readily isolated in 34% yield. All the structures of the final products as well as key intermediates were entirely consistent with the ^{1}H NMR and LC-MS spectra (see Supporting Information).

Biological evaluation

Dox is undoubtedly one of the most commonly used anti-cancer therapeutics, and due to the inherent fluorescence, it is widely applied as a convenient analytical/visualization tool in different biological trials. Thus, upon Dox treatment, fluorescence imaging of cells reveals its micro-distribution within the intracellular compartment. Therefore, this drug molecule is an excellent and versatile theranostic agent.[53] The synthesized conjugates 17 and 20, as well as unmodified Dox, have been thoroughly evaluated against LNCaP cells, which were used as PSMA positive line and vs. PC-3 cells used as PSMA negative control. The detailed experimental protocol is presented in Supporting Materials in detail.

Firstly, we have evaluated the penetration ability and selectivity of fluorescent conjugate **36** modified with PSMA vector toward LNCaP and PC-3 cells using fluorescent microscopy. We observed a homogeneous diffuse staining of LNCaP cells cytoplasm after 2 h incubation with the compound (Figure 1a). In contrast, no fluorescent signal of Cy5 dye was determined in the case of PC-3 cells (Figure 1b). We can, therefore, speculate that the designed vector can be used for the targeted drug delivery at least in PSMA-overexpressed LNCaP cells.

The preliminary results of a comparative analysis of intracellular localization and selectivity of the designed compounds are presented in Figure 2. As clearly shown in Figure 2, Dox was specifically localized

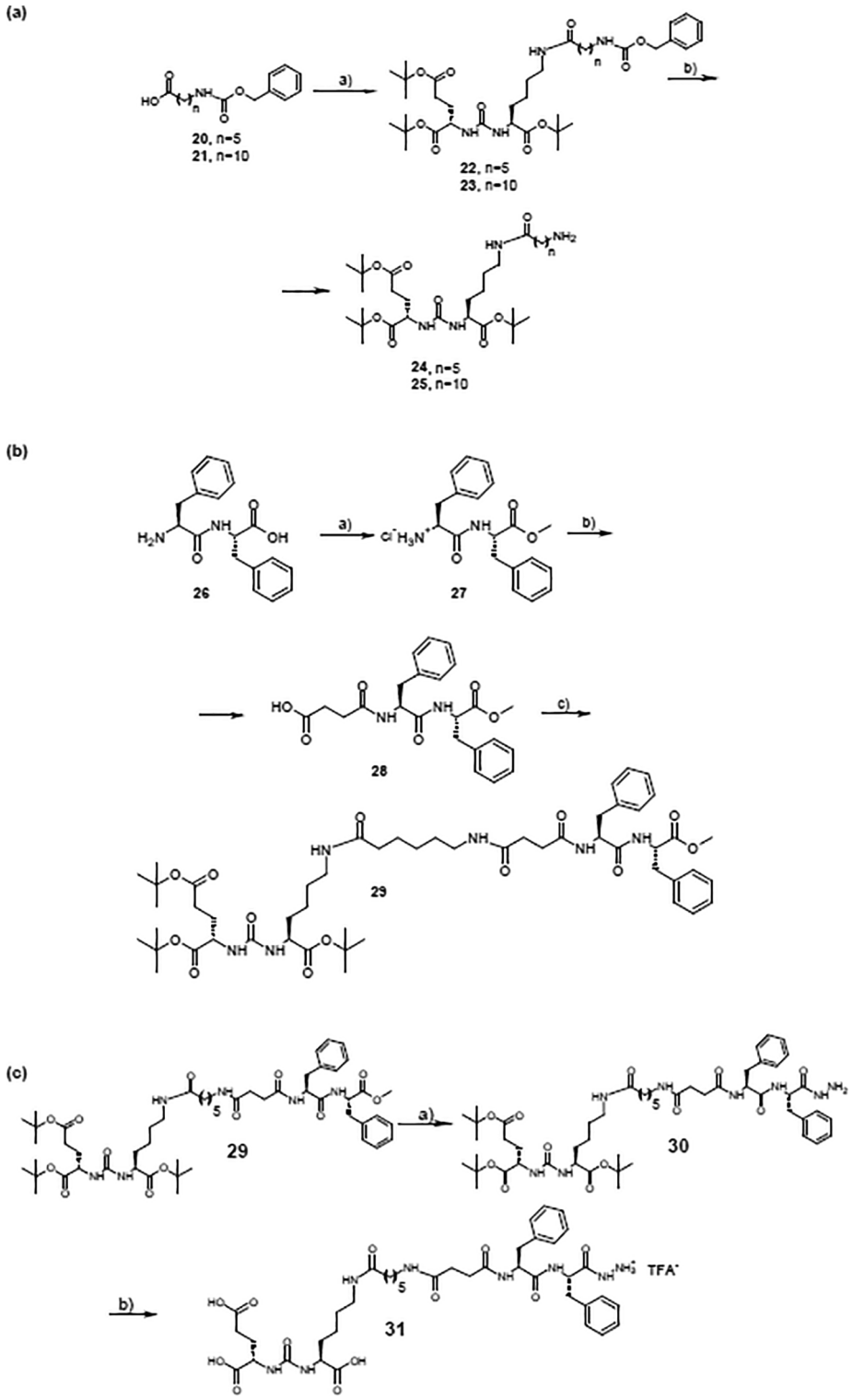

Scheme 3. Synthesis of *bi*-phenylalanine-containing ligands **33** and **34**: (**a**) *a*) HBTU, HOBt and DIPEA, yield **22**–61%, **23**–66%; *b)* H_2, 10% Pd/C, CH_2Cl_2, yield **24**–97%, **25**–99% (**b**) *a*) $SOCl_2$, MeOH, yield **27**–76%, *b)* DIPEA, succinic anhydride, HBTU, HOBT and DIPEA, yield **28**–94%, c) HBTU, HOBt and DIPEA, yield **29**–56%, (**c**) *a*) MeOH, Δ, an excess of N_2H_4 H_2O, yield **30**–96%; *b*) TFA (90%)/MeOH, yield **31** 96%

within the nuclei either in LNCaP or PC-3 cells. The accumulation of conjugates inside the cell nuclei and cytoplasm was investigated at 40 ms exposure (Figure 3). Trace amount of the drug was detected in the cell cytoplasm as well. However, the fluorescence intensity of Dox in the cytoplasm of LNCaP cells was 3.5 times less than in nucleus and 3.7 times less in the case of PC-3 culture. Compound **32** with the shorter linker was predominately deposited in nuclei and within the cytoplasm, instead of compound **33** which was spread smoothly mainly beyond nuclei. The best compartmentalization was revealed for compound **34** equipped by two phenylalanine fragments. Thus, the molecule was localized primary in the nuclei of LNCaP cells thereby providing a drastic selectivity in contrast to Dox. Presumably, in addition to possible passive diffusion, it could be due to a relative instability of the trigger under the assay conditions. As a result, the unbounded amount of Dox

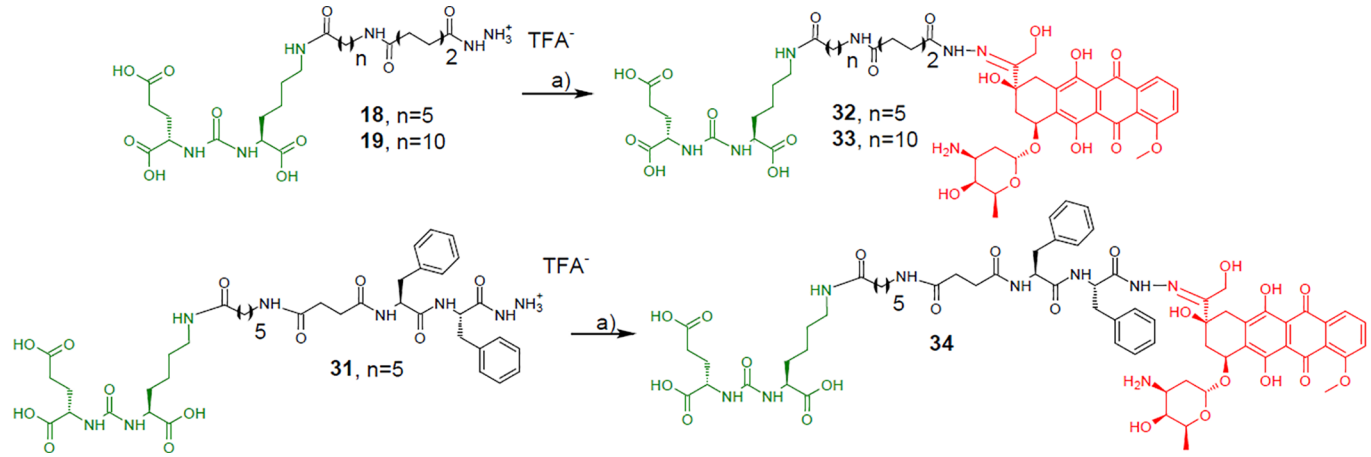

Scheme 4. Synthesis of doxorubicin conjugates: a) doxorubicin hydrochloride, TFA, MeOH, yields: **32**–16%, **33**–17%, **34**–13% (the core-head is marked in green, and drug – in red).

penetrated the outer cell membrane after 2 h incubation. A relatively minor effect was observed for the tested compounds in PC-3 cells except unselective Dox. It should be especially noted that the covalent conjugate **37** did not release the active substance at all. It can be related to high stability of amide bond which is insensitive to amidase-driven cleavage. An extremely poor amount of Dox was detected in the nuclei of both cell lines used. Nevertheless, we speculate that compound **37** penetrated LNCaP as well as PC-3 cell walls via passive transport. The imaging procedure was also performed for these samples after 48 h (see Supporting Information). Doxorubicin fluorescence was detected mostly in nuclei with unmodified Dox and conjugate **34**, and in the cytoplasm in the case of compound **37** (see Supporting Information).

All the synthesized conjugates (**32–34** and **37**) as well as unmodified Dox have been thoroughly evaluated in LNCaP cells which were used as PSMA positive line and in PC-3 cells used as PSMA negative control (see Supporting Information). Anti-cancer potency of the novel doxorubicin conjugates 32–34 as well as 37 had been assessed in the standard MTT test (Table 1). As shown in Table 1 and Figure 4, the most active compound from this series demonstrated a CC_{50} value of 95 nM close to that observed for doxorubicin (CC_{50} = 93 nM). Low concentrations of conjugate **34** exhibited significant cytotoxicity against LNCaP cells comparable to Dox (Figure 4a). Conjugates **32** (CC_{50} = 331 nM) and **33** (CC_{50} = 487 nM) demonstrated less activity against tumor cells than compound **34**. At the same time, an CC_{50} value of conjugate **34** against PC-3 cells was 926 nM as compared to Dox (CC_{50} > 500 nM). Therefore, the selectivity index of compound **34** was close to 5 towards LNCaP in contrast to unselective Dox. Conjugate **37** did not cause any cytotoxic effect on both cell lines at the same and some upper concentrations. It should be especially noted that the obtained results correlate well with the data published previously for an analogous Dox-contained conjugate by Jayaprakash and colleagues[52]. The authors used similar amide adjustment point which was hoped to be cleaved by an amidase inside the cell, however poor cytotoxicity was observed against PSMA-positive C4-2 and PSMA-negative PC-3 prostate cancer cells using the colorimetric CellTiter 96 Aqueous Cell Proliferation Assay in contrast to the unmodified Dox (IC_{50} > 32 nM). The hydrolysis kinetics of compound **34** at different pH values are presented in Supporting Information (Figure S1). We also estimated the inhibition efficiency of compound **29** (without *t*-Bu protecting groups) as well as DUPA against GCPII (Figure S2).

Thus, MTT assay has revealed conjugate **34** as more toxic against the selected cultures than compound **37** because of its ability to release Dox inside the cells, and more selective than unbounded Dox (Figure 4b).

Data were obtained in three independent experiments. Plotting and calculation of the standard deviation (SD) value were made using Microsoft Office Excel 2007 software. Data were analyzed using the Analysis of Variance (ANOVA) test and Post-Hoc test was performed (the assessment of statistical significance is presented in Supporting Information). P values < 0.05 were considered significant.

In vivo evaluation

To perform a preliminary *in vivo* study the lentiviral transfection of

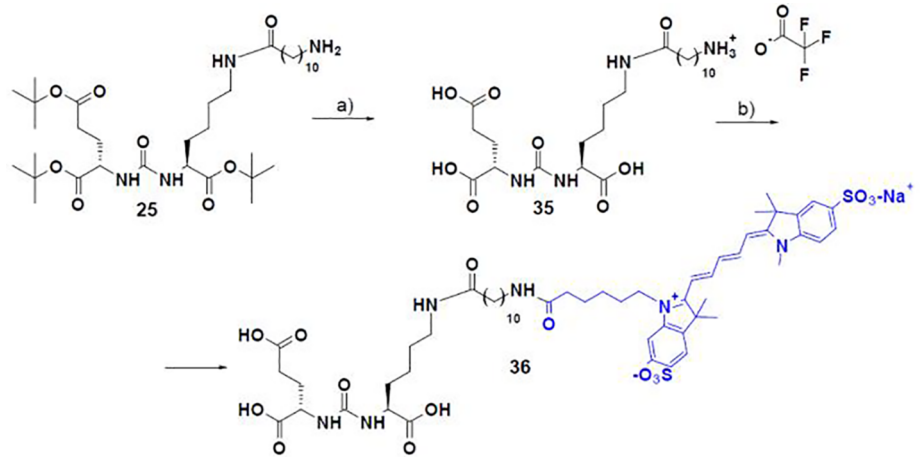

Scheme 5. Synthesis of the fluorescent conjugate **36**: *a*) 10% TFA in DCM, yield 98% *b*) Sulfo-Cy5-NHS ester, DIPEA, DMF, yield 30%

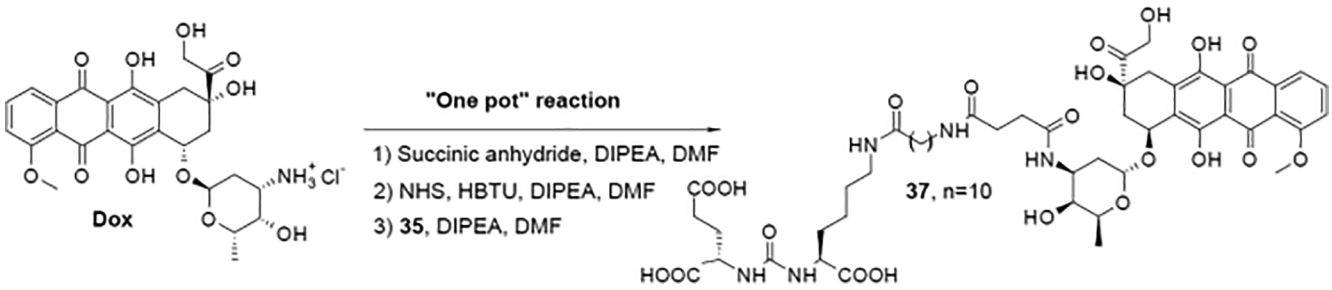

Scheme 6. Synthesis of the stable Dox-conjugate **37**.

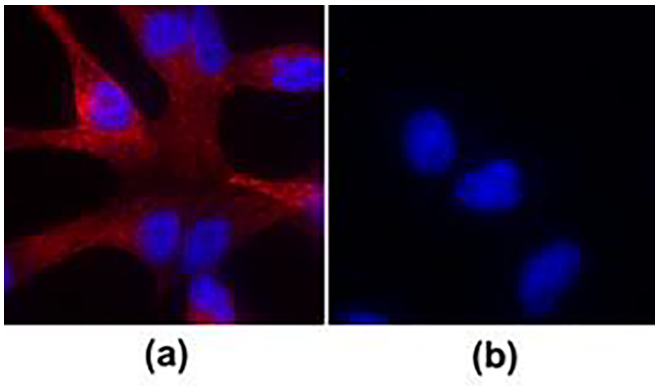

Fig. 1. Binding potency and internalization of the fluorescent conjugate 36 into LNCaP (a) and PC-3 (b) cells after 2 h co-incubation. Cells nuclei are stained with DAPI (*blue*, 4′,6-diamidino-2-phenylindole is a fluorescent stain that binds strongly to DNA).

PC-3 cells was carried out using pseudotyping VSV-G vector. As a result, following the procedure described by

Chang and co-workers[7] we have obtained the PC3-PIP(PSMA +) line expressed PSMA vector. This line was subsequently inoculated s.c. into nu/nu mice to obtain xenograft *in vivo* model. This model was used to assess the efficiency of the designed conjugate **34** and Dox. The samples were administered i.p. at a weekly dose of 4 mg/kg for 3 weeks, while PBS was used as a negative control. Tumor size at the end of the study was estimated manually. Mice treated with conjugate **34** have demonstrated improved food consumption and less weight loss. The obtained results are shown in Figure S4. Thus, Dox showed the best results and TGI^{av} ~92%, while the conjugate demonstrated TGI^{av} ~ 65% (the initial tumor size was 4 mm).

In silico modeling

Currently, a large amount of X-Ray data on structure of PSMA with various small-molecule ligands is available within the PDB databank.[54] In silico modelling was performed in ICM-Pro Software (v.3.8–3)[55] using the crystallographic structure published previously by Ganguly and colleagues[56] (PDB code: 4JYW). It was used as the most appropriate 3D template as the molecule inside contained both the core-head attached by a linker of similar length to our compounds as well as the aromatic fragment positioned at the entrance of the tunnel. The pre-identified binding site was completely reconstructed without any flexible points although conservative water molecules identified by the alignment of several crystals, including 4JYW, 2XEG, 3D7D, and 4NGQ, were retained. After the site was built the model was internally validated. Thus, the reference compound was then docked into the binding pocket as 2D structure, keeping the native stereo-specificity, using the common force-field function shared in the software; this includes H-bonding, hydrophobic, ionic, dipole-dipole, π-cationic, coordination and stacking terms. At the output, 25 possible conformations were generated. Subsequently, the structures of the conjugates have been evaluated *in silico* using the developed 3D model. Docking procedure was performed using a batch mode available in ICM-Pro Software with the appropriate settings determined during the validation step described previously. On average, 30 different conformations were generated for each structure tested. The best conformations were identified on the basis of a thorough visual inspection and energetic score values.

Docking procedure (Figure 5) was performed through a batch mode in ICM-Pro Software keeping the appropriate settings determined during the validation step described previously. On average, 35 different conformations were generated for the each molecule tested. The best conformations were identified on the basis of thorough visual inspection and score values. For example, the predicted binding mode for the most active compound **34** as well as 3D alignment with the ref. molecule are presented in Fig. 3a. A comparative analysis of the supramolecular interface is discussed in more detail below (*see the Discussion Section*).

Discussion

The clinical application of many anticancer drugs, including Dox, is unavoidably limited because of a poor target selectivity and off-target systemic toxicity, particularly cardiotoxicity and immunosuppression.[57] The targeted drug delivery has several advantages over existing chemotherapy regimens due to a drug molecule is transported specifically to the cancer nest thereby minimizing adverse side effects and lowering the administered dose.[58–60] From this point of view, PSMA is unambiguously among the most attractive drug targets as it is abundantly expressed in PC over other cells, constitutively endocytosed and contains druggable binding sites. Twelve molecules have been evaluated in different clinical trials as diagnostic tools. The most advanced compounds I^{123}-Iofolastat,[61] Technetium^{99m}Tc-trofolastat[62] and^{68}Ga-PSMA[63] are undergoing Phase II/III evaluation. An ongoing study in Australia has recruited 200 patients to determine the activity of PSMA-based RLT with cabazitaxel and the effects on PSA response rate.[64] To our intense disappointment, there is still only one drug conjugate in clinics for PSMA-targeted drug delivery. EC-1169 by Endocyte is a drug conjugate consisting of tubulysin B hydrazide, a tubulin polymerization inhibitor, DUPA-containing warhead, and degradable disulfide and carbamate moieties.[65] The product is in early clinical development for the treatment of metastatic castration-resistant PC.[66] The main drawbacks include: a) generally, a relatively modest anti-cancer efficiency *in vivo* as compared to an unmodified drug molecule due to a range of reasons, e.g.: a) weak release capacity; b) the spacer length and topology are still beyond benefit conditions, c) a relatively poor pharmacokinetic profile, and d) applied clinical protocols are rather beyond of real clinical success. To properly address these issues, several approaches have recently been considered as the most prominent: a) drug release should be improved by morphing the linker area and the optimization of a junction with reduced off-target drug losses, b) spacer should have an appropriate length and substituents along the tail to provide good binding affinity and selectivity, c) PK parameters should also be improved to develop a convenient, stable and effective drug

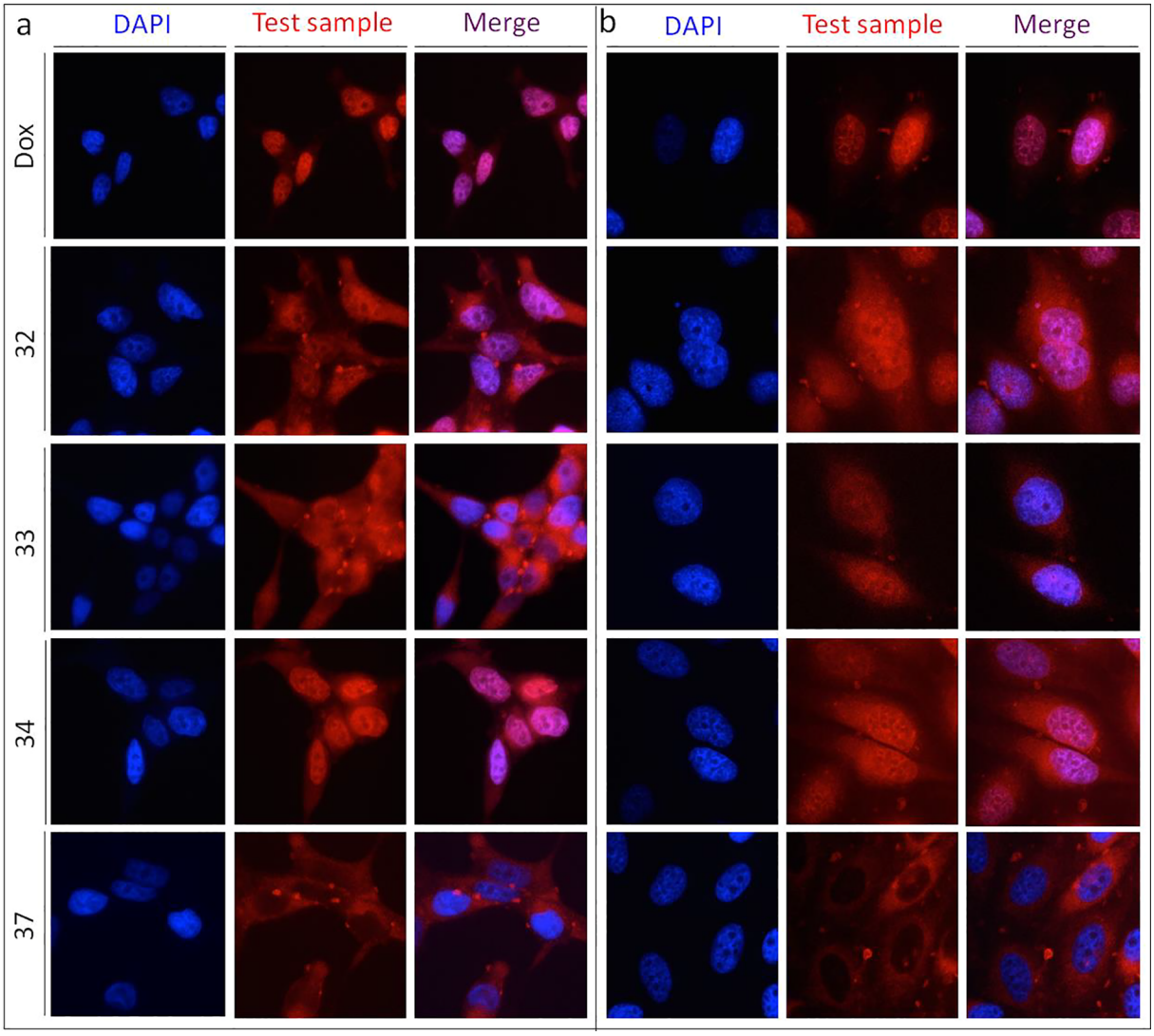

Fig. 2. Selectivity profile and intracellular localization of the synthesized molecules (15 μM) towards LNCaP and PC3 cell lines (after 2 h of inoculation).

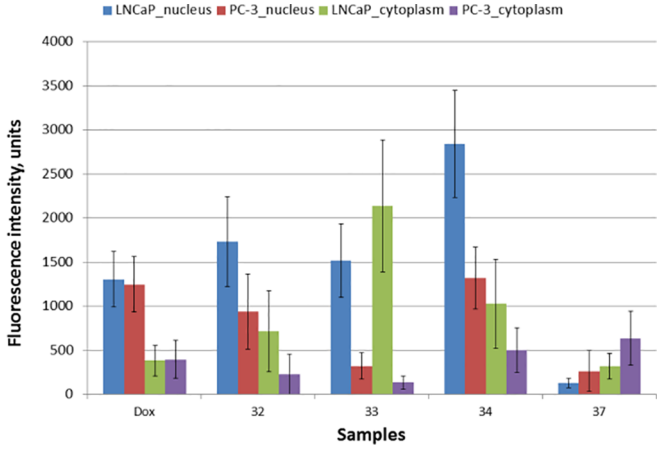

Fig. 3. Accumulation level for conjugates **32–34**, **37** in LNCaP and PC3 cells. Results are shown as means ± SD, ** $p < 0.01$ (one-way ANOVA).

formulation.

In the present work, we used one of the most promising urea-based core containing lysine functionality as the main focus was placed rather on the linker length and drug attachment point. However, in addition to a well-known Glu-Urea-Glu head, several other «locomotives» over phosphinate-, phosphonate- and thiol-containing ligands have also been developed for the PCa-targeted drug delivery and diagnostics.

Table 1
Anti-cancer potency of the synthesized conjugates.

Compounds	CC_{50}, nM*	
	LNCaP	PC-3
32	331 ± 15	2068 ± 323
33	487 ± 35	2791 ± 914
34	95 ± 11	926 ± 76
37	na**	na**
Dox	106.6 ± 5	< 500

* the compounds were tested independently three times.
** not active.

The experimental achievements described above as well as the performed *in silico* modelling (see *In Silico* Modeling Section) approached us to design novel PSMA-selective small-molecule conjugates attempting to properly address the issues listed above. As a result, we demonstrated that a flexible poly-alkyl linker, exemplified particularly by moderate chain-length (n = 5), did contribute to the activity providing not much lesser *in vitro* effect as compared to the parent drug

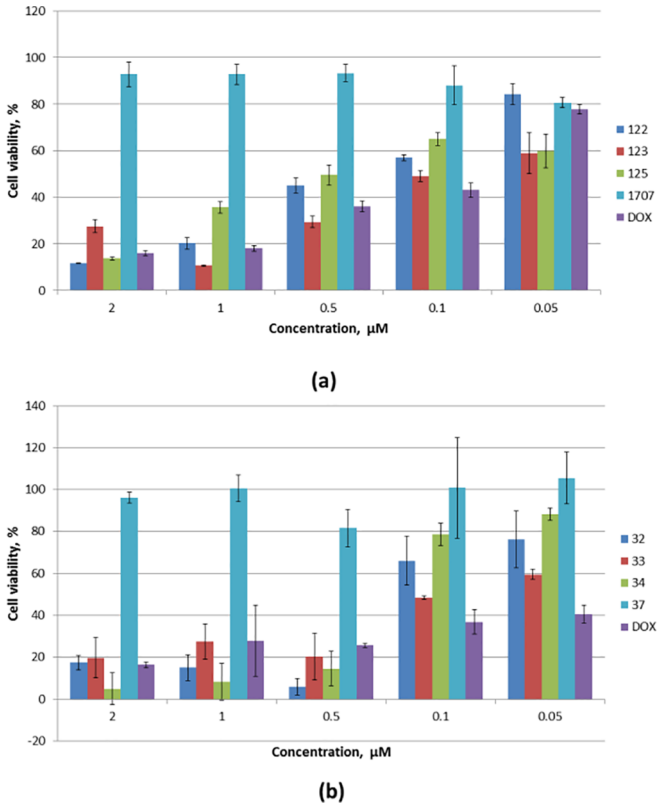

Fig. 4. Cytotoxicity of conjugates **32**–**34**, **37** and Dox against LNCaP (**a**) and PC-3 (**b**) cells.

molecule. Indeed, compound **34** demonstrated good drug release and accumulation in nuclei of LNCaP cells after 2 h incubation comparable with the unmodified Dox. Conjugate **37** did not release the drug at all, thereby discouraging Dox penetration in the cell nucleus under the same conditions. We also synthesized and evaluated a similar conjugate **32** and **33**, however, it showed the internalization potency and activity several times lower than compound **34**. Therefore, we can conclude that the linker in the structure of compound **34** is more appropriate for the targeted drug delivery and contains an appropriate trigger.

Presumably, the properties of the selected drug molecule greatly affect the mechanism of transport cuz the analogues PSMA-vector equipped by Cy5 showed an outstanding specificity. Compound **34** can penetrate PC-3 cell wall simply via passive transport. This case, Dox may play a driver role or influences the spatial geometry of the whole molecule making it more amenable for diffusion. Moreover, penetration may occur due to a partial hydrolysis of azo-bound outside the cells under the applied assay conditions during the time. We also suggest that conjugate **34** penetrate PC-3 membrane via non PSMA-maintained endocytosis. Actually, this stage was a relatively slow and we detected the sustained accumulation of the compound within the cytoplasm. Dox was rapidly concentrated in the nuclei in contrast to compound **34**. The rate of hydrolysis is one of the possible reasons responsible for this difference. According to the hydrolysis rate of conjugate **34** at pH = 7.4, it is going to be stable to pH-dependent hydrolysis in blood due to its slightly basic pH range of 7.35–7.45 (Figure S1), but further investigations of stability and distribution of the conjugate *in vivo* are needed.

The results obtained during MTT assay also confirmed that conjugate **34** is more appropriate for the targeted drug delivery in contrast to other compounds. Indeed, the most promising compound form our series attenuated the growth of LNCaP cells with a CC_{50} value of 95 nM close to that observed for Dox. However, the conjugates bearing the spacers of 6-aminohexanoic or 11-aminoundecanoic acids were far less active (CC_{50} = 331 and 487 nM, respectively) as compared to the hybrids containing *bi*-phenylalanine linker or Dox itself (CC_{50} = 93 nM).

The principal role of the aromatic inclusions in binding, usually yielding more active compounds, was elucidated *in silico* on the basis of the results outputted from 3D molecular docking study. As clearly shown in Figure 5, compound **34**, without Dox as it has presumably no impact on binding, has a very similar location of the core-head in close proximity to the template molecule thereby providing a tight coordination bond with Zn^{2+} via its urea oxygen as well as hydrogen bond with Y552, while the vicinal amine fragments provide two H-bonds with the backbone oxygen of G518. Glutamate fragment is the most crucial for good binding affinity and strongly anchored within the active site by the ensemble of K699, N257, W381 and R210. By analogy to other urea-containing PSMA ligands, the carboxylic group of lysine moiety provides H-bond with R536, while the amide joint between the core-head and the linker forms two H-bonds with R534 and S517. The second linker amide bond between 6-aminohexanoic and adipic acids forms a weak H-bond with D465. Instead of ligands which were designed to catch the double π-stacking with R536 and R534, e.g. 3D7D and 4NGQ, thereby forming a 'sandwich' structure, the terminal phenylalanine fragment of molecule **34** provides *t*-shaped stacking with W541, while the position of the second aromatic moiety is the same as it has recently been uncovered for the ref. ligand. This fragment interacts with S501 (Ser—O—H Phe-ligand). In general, the architecture of the whole supramolecular interface correlates well with that observed in the selected ref. crystal. A relatively good overlapping (RMSD = 0.47) was observed between the active conformation of our compound and the template molecule, particularly within the active site and at the entrance of the tunnel. In addition, intramolecular peptide-based H-bond was observed between these two phenylalanine residues thereby forming a stable γ-like turn. With regard to the score function, the most reliable conformation of the ref. molecule yielded an E^{score} value of −102 kcal/mol similar to that predicted for the carrier **34**, E = -105 kcal/mol. It should be especially noted that similar to the strategy applied by Ganguly and co-workers[56] and the reports cited above, we observed a significant gain in penetration as aromatic binding points were introduced into the linker frame.

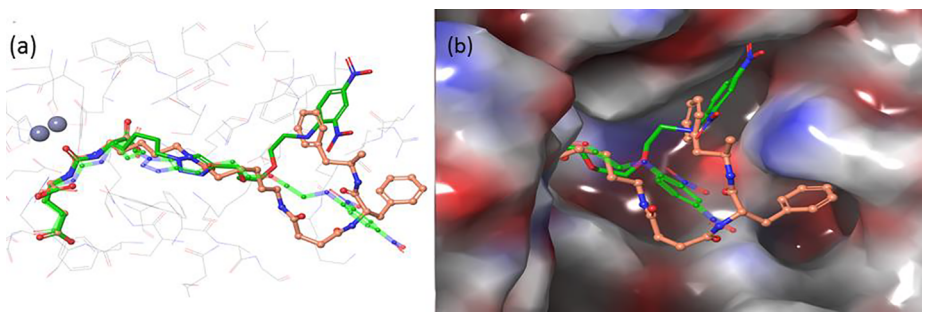

Fig. 5. The predicted binding mode for the most active conjugate **34**: (*a*) the superposition of compound **34** (*yellow*, docking results) with the ref. molecule (*orange*, X-Ray data); (*b*) the localization of compound **34** inside the tunnel.

With respect to the drug attachment point, we speculate that azo-moiety introduced in our compounds can be more liable towards the hydrolytic cleavage or/and hydrolase-driven destruction vs. amide joint suggested by Jayaprakash and colleagues.[52] As clearly shown in Table 1, conjugate **34** did release the active substance in LNCaP cells but also was localized within the cytoplasm, while compound **37** did not release Dox at all and was predominantly deposited in cytoplasm hence it was ineffective *de facto* in both cell lines. Indeed, although this modification does provide some benefits at the sites of targeting, the stability of such conjugates in plasma should be clearly addressed during further evaluation. In addition, we are now planning to introduce additional aromatic fragments and other triggers, e.g. ester group, into the conjugate to improve the target activity and subsequently evaluate the most promising conjugates *in vivo*.

In conclusion, we have synthesized and evaluated four novel PSMA-specific drug conjugates equipped with Dox. The selected drug molecule was attached to the selected vector via bio-degradable azo-linker or stable amide bond. It was revealed that the most active conjugate **34** readily released Dox inside the cells in contrast to other analogue. Additionally, compound **34** has approximately the same level of activity against LNCaP cells as Dox (CC_{50} value of 95 nM and 93 nM, respectively). Anyhow, compound **34** can be used as a convenient starting point appropriate for the follow up optimization study.

As largely substantiated by a plethora of recent preclinical and clinical findings, PSMA can be reasonably regarded as a promising target for the targeted drug delivery and diagnostics thereby providing novel therapeutic approaches, including small-molecule anti-cancer drug conjugates, PSMA-based aptamers, peptides, modified antibodies, as well as radiotherapy and immunotherapy. Certainly, it holds a unique promise of getting mainstream success as an ideal biological target for PCa-specific imaging and drug therapy. Its successful preliminary performance, clearly elucidated during different clinical trials and scenarios as well as valuable ability to detect lesions even in relatively low PSA values, is fairly attractive and reliable to be advanced in clinics further. Taking into account that through the last decade intensive research programs within this field have been launched and heavily promoted, the first-*in*-class PSMA-targeted drug conjugates will reach clinical trials soon.

Acknowledgments

Authors thanking Dr. I. Minn for consultations about GCPII activity test. The authors would like to kindly acknowledge the Ministry of Education and Science of the Russian Federation, government grant 20.9907.2017/VU (expert opinion, discussion, and manuscript preparation), 17-14-01316 (psma synthesis) and Russian Science Foundation №17-74-30012, IBG RAS Ufa (biological evaluation and compound selection).

Appendix A. Supplementary data

Supplementary data to this article can be found online at https://doi.org/10.1016/j.bmcl.2019.01.040.

References

1. Cancer Research UK. Cancer risk. https://www.cancerresearchuk.org/health-professional/cancer-statistics/risk.
2. Ferlay J, Soerjomataram II, Dikshit R, et al. *Int J Cancer.* 2014;136:E359–E386. https://doi.org/10.1002/ijc.29210.
3. American Cancer Society. https://www.cancer.org.
4. Ceci F, Castellucci P, Cerci JJ, Fanti S. *Methods.* 2017;130:36–41. https://doi.org/10.1016/j.ymeth.2017.07.009.
5. Ceci F, Herrmann K, Hadaschik B, Castellucci P, Fanti S. *Eur J Nucl Med Mol Imaging.* 2017;44:78–83. https://doi.org/10.1007/s00259-017-3723-3.
6. Haffner MC, Kronberger IE, Ross JS, et al. *Hum Pathol.* 2009;40:1754–1761. https://doi.org/10.1016/j.humpath.2009.06.003.
7. Chang SS, Reuter VE, Heston WD, Bander NH, Grauer LS, Gaudin PB. *Cancer Res.* 1999;59:3192–3198.
8. de Bono JS, Oudard S, Ozguroglu M, et al. TROPIC Investigators. *Lancet (London, England).* 2010;376:1147–1154. https://doi.org/10.1016/S0140-6736(10)61389-X.
9. Attard G, Parker C, Eeles RA, et al. *Lancet (London, England).* 2016;387:70–82. https://doi.org/10.1016/S0140-6736(14)61947-4.
10. Rhee H, Gunter JH, Heathcote P, et al. *BJU Int.* 2015;115(Suppl):3–13. https://doi.org/10.1111/bju.12964.
11. Foss CA, Mease RC, Cho SY, Kim HJ, Pomper MG. *Curr Med Chem.* 2012;19:1346–1359. https://doi.org/10.2174/092986712799462612.
12. Santoni M, Scarpelli M, Mazzucchelli R, et al. *J Biol Regul Homeost Agents.* 2014;28:555–563.
13. Ghosh A, Heston WD. *J Cell Biochem.* 2004;91:528–539. https://doi.org/10.1002/jcb.10661.
14. Eiber M, Fendler WP, Rowe SP, et al. *J Nucl Med.* 2017;58:67–76. https://doi.org/10.2967/jnumed.116.186767.
15. Tagawa ST, Batra J, Vallabhajosula S. *52nd Annu Meet Am Soc, Clin Oncol.* 2016.
16. Fernández-García EM, Vera-Badillo FE, Perez-Valderrama B, Matos-Pita AS, Duran I. *Clin Transl Oncol.* 2015;17:339–357. https://doi.org/10.1007/s12094-014-1259-6.
17. Fendler WP, Rahbar K, Herrmann K, Kratochwil C, Eiber M. *J Nucl Med.* 2017;58:1196–1200. https://doi.org/10.2967/jnumed.117.191023.
18. Rahbar K, Ahmadzadehfar H, Kratochwil C, et al. *J Nucl Med.* 2017;58:85–90. https://doi.org/10.2967/jnumed.116.183194.
19. Hadaschik BA, Boegemann M. *J Nucl Med.* 2017;58:1207–1209. https://doi.org/10.2967/jnumed.117.194753.
20. von Eyben FE, Roviello G, Kiljunen T, et al. *Eur J Nucl Med Mol Imaging.* 2018;45:496–508. https://doi.org/10.1007/s00259-017-3895-x.
21. von Eyben FE, Kiljunen T, Joensuu T, Kairemo K, Uprimny C, Virgolini I. *Oncotarget.* 2017;8:66112–66116. https://doi.org/10.18632/oncotarget.19805.
22. Roy J, Nguyen TX, Kanduluru AK, et al. *J Med Chem.* 2015;58:3094–3103. https://doi.org/10.1021/jm5018384.
23. Tagawa ST, Beltran H, Vallabhajosula S, et al. *Cancer.* 2010;116:1075–1083. https://doi.org/10.1002/cncr.24795.
24. Ristau BT, O'Keefe DS, Bacich DJ. *Urol. Oncol.* 2014;32:272–279. https://doi.org/10.1016/j.urolonc.2013.09.003.
25. Chang WY, Kao HW, Wang HE, et al. *Bioorganic Med Chem Lett.* 2013;23:6486–6491. https://doi.org/10.1016/j.bmcl.2013.09.012.
26. Kovar JL, Cheung LL, Simpson MA, Olive DM. Prostate Cancer. 2014;104248. doi:10.1155/2014/104248.
27. Mease RC, Foss CA, Pomper MG. *Curr Top Med Chem.* 2013;13:951–962. https://doi.org/10.2174/1568026611313080008.
28. Morris MJ, Divgi CR, Pandit-Taskar N, et al. *Clin Cancer Res.* 2005;11:7454–7461. https://doi.org/10.1158/1078-0432.CCR-05-0826.
29. Galsky MD, Eisenberger M, Moore-Cooper S, et al. *J Clin Oncol.* 2008;26:2147–2154. https://doi.org/10.1200/JCO.2007.15.0532.
30. Bander NH, Milowsky MI, Nanus DM, Kostakoglu L, Vallabhajosula S, Goldsmith SJ. *J Clin Oncol.* 2005;23:4591–4601. https://doi.org/10.1158/1078-0432.CCR-1004-0023.
31. Tagawa ST, Milowsky MI, Morris M, et al. *Clin Cancer Res.* 2013;19:5182–5191. https://doi.org/10.1158/1078-0432.CCR-13-0231.
32. Murga JD, Moorji SM, Han AQ, Magargal WW, DiPippo VA, Olson WC. *Prostate.* 2015;75:242–254. https://doi.org/10.1002/pros.22910.
33. Herrmann K, Bluemel C, Weineisen M, et al. *J Nucl Med.* 2015;56:855–861. https://doi.org/10.2967/jnumed.115.156133.
34. Martin SE, Ganguly T, Munske GR, et al. *Bioconjug Chem.* 2014;25:1752–1760. https://doi.org/10.1021/bc500362n.
35. Tykvart J, Schimer J, Jančařík A, et al. *J Med Chem.* 2015;58:4357–4363. https://doi.org/10.1021/acs.jmedchem.5b00278.
36. Schwenck J, Tabatabai G, Skardelly M, et al. *Eur J Nucl Med Mol Imaging.* 2015;42:170–171. https://doi.org/10.1007/s00259-014-2921-5.
37. Afshar-Oromieh A, Zechmann CM, Malcher A, et al. *Eur J Nucl Med Mol Imaging.* 2014;41:11–20. https://doi.org/10.1007/s00259-013-2525-5.
38. Vallabhajosula S, Nikolopoulou A, Babich JW, et al. *J Nucl Med.* 2014;55:1791–1798. https://doi.org/10.2967/jnumed.114.140426.
39. Viola-Villegas NT, Sevak KK, Carlin SD, et al. *Mol Pharm.* 2014;11:3965–3973. https://doi.org/10.1021/mp500164r.
40. Tolmachev V, Malmberg J, Estrada S, Eriksson O, Orlova A. *Int J Oncol.* 2014;44:1998–2008. https://doi.org/10.3892/ijo.2014.2376.
41. Bandari RP, Jiang Z, Reynolds TS, et al. *Nucl Med Biol.* 2014;41:355–363. https://doi.org/10.1016/j.nucmedbio.2014.01.001.
42. Osborne JR, Green DA, Spratt DE, et al. *J Urol.* 2014;191:1439–1445. https://doi.org/10.1016/j.juro.2013.10.041.
43. El-Zaria ME, Genady AR, Janzen N, Petlura CI, Beckford DR, Valliant JF. *Dalton Trans.* 2014;43:4950–4961. https://doi.org/10.1039/c3dt53189a.
44. Olson WC, Israel RJ. Front. Biosci. (Landmark Ed). 2014;19:12–33. doi:10.2741/4193.
45. Cho SY, Gage KL, Mease RC, et al. *J Nucl Med.* 2012;53:1883–1891. https://doi.org/10.2967/jnumed.
46. Eiber M, Maurer T, Souvatzoglou M, et al. *J Nucl Med.* 2015;56:668–674. https://doi.org/10.2967/jnumed.115.154153.
47. Chatalic KLS, Veldhoven-Zweistra J, Bolkestein M, et al. *J Nucl Med.* 2015;56:1094–1099. https://doi.org/10.2967/jnumed.115.156729.
48. Shallal HM, Minn I, Banerjee SR, Lisok A, Mease RC, Pomper MG. *Bioconjug Chem.* 2014;25:393–405. https://doi.org/10.1021/bc4005377.
49. Tykvart J, Schimer J, Bařinková J, et al. *Bioorg Med Chem.* 2014;22:4099–4108. https://doi.org/10.1016/j.bmc.2014.05.061.
50. Barinka C, Byun Y, Dusich CL, et al. *J Med Chem.* 2008;51:7737–7743. https://doi.

org/10.1021/jm800765e.
51. Maresca KP, Hillier SM, Femia FJ, et al. *J Med Chem.* 2009;52:347–357. https://doi.org/10.1021/jm800994j.
52. Jayaprakash S, Wang X, Heston WD, Kozikowski AP. *ChemMedChem.* 2006;1:299–302. https://doi.org/10.1002/cmdc.200500044.
53. Mohan P, Rapoport N. *Mol Pharm.* 2010;7:1959–1973.
54. RCSB Protein Data Bank. https://www.rcsb.org.
55. ICM-Pro Software. http://www.molsoft.com/icm_pro.html.
56. Ganguly T, Dannoon S, Hopkins MR, et al. *Nucl Med Biol.* 2015;42:780–787. https://doi.org/10.1016/j.nucmedbio.2015.06.003.
57. Raghavan D, Koczwara B, Javle M. *Eur J Cancer.* 1997;33:566–574. https://doi.org/10.1016/S0959-8049(96)00510-2.
58. DeFeo-Jones D, Brady SF, Feng DM, et al. *Mol Cancer Ther.* 2002;1:451–459.
59. DeFeo-Jones D, Garsky VM, Wong BK, et al. *Nat Med.* 2000;6:1248–1252. https://doi.org/10.1038/81351.
60. Khan SR, Denmeade SR. *Prostate.* 2000;45:80–83.
61. Babich J, Coleman ER, Heertum RV, et al. *Soc Nucl Med.* 2012;Vol:53.
62. NCT01667536 A service of the U.S. National Institutes of Health. https://www.clinicaltrials.gov/ct2/show/NCT01667536.
63. NCT02282137 A service of the U.S. National Institutes of Health. https://clinicaltrials.gov/ct2/show/NCT02282137.
64. NCT03392428 A service of the U.S. National Institutes of Health. https://clinicaltrials.gov/ct2/show/NCT03392428.
65. Morris MJ, Vogelzang NJ, Sartor O, et al. *Ann Oncol.* 2016;27.. https://doi.org/10.1093/annonc/mdw372.
66. NCT02202447 A service of the U.S. National Institutes of Health. https://clinicaltrials.gov/ct2/show/NCT02202447.